Reheating Process of Metal Matrix Composites for Thixoforming and Their Inductive Coil Design

C.G. Kang, S.W. Youn, and P.K. Seo

(Submitted 1 June 2001; in revised form 16 October 2001)

In this work, the fabrication processes of particulate metal matrix composites (PMMCs) with a homogeneous distribution of reinforcement and their reheating for thixoforming were studied. Electromagnetic stirring was used to fabricate PMMCs to vary particle size. PMMCs were tested before and after the reheating process using a tensile test with and without heat treatment. The combined process conditions for fabricating the PMMCs are also suggested for a variety of particle sizes. For the thixoforming of PMMCs, fabricated billets are reheated by using an induction heating system with a maximum capacity of 20 kW. The effects of the dispersion state of the reinforcements on the reheating temperature and microstructural morphology were investigated.

Keywords dispersion state, inductive coil design, metal matrix composites, particle size, reheating process, thixoforming

1. Introduction

Improving fuel efficiency in the transportation fields, such as automotive, vessel, and aircraft, is an important topic from an environmental point of view. From this perspective, the process of manufacturing lightweight products coinciding with the requirements of the parts must be developed.[1-11] This need to reduce transportation weight has led to a major increase in the production of metal matrix composite (MMC) engine parts for automotive applications. Therefore, many studies on the MMCs have been actively performed. The process of manufacturing MMC parts by thixoforming is a very promising technology for manufacturing net-shape products at a relatively low cost.

Particulate-reinforced MMCs (PMMCs) combine metallic properties, such as toughness and ductility, with ceramic properties, such as high strength wear resistance and high modulus, leading to superior strength in shear and compression. A 50% increase in modulus, achieved by substituting a discontinuous silicon carbide-reinforced aluminum matrix composite for an unreinforced wrought aluminum alloy, resulted in a 10% reduction in weight.[12-14]

The fabrication method of MMCs by the squeeze-casting process has some problems, including the homogeneous dispersion of the particulate's extensive interfacial reactions and particulate fracturing during mechanical stirring,[15,16] In comparison, the powder metallurgy method makes it easy to disperse the reinforcements homogeneously and to control interfacial reaction.[17] However, the squeeze-casting process is lower in cost and is nearer to net-shape manufacturing than powder metallurgy.[18]

As a solution to improving the mechanical properties and to reducing manufacturing costs, PMMCs provide an opportunity for thixoforming, which is one of the processes manufacturing net-shaped components. In this work, both mechanical stirring and electromagnetic stirring were used to fabricate PMMCs to

Table 1 Chemical Composition of A357

Content	Si	Fe	Cu	Mn	Mg	Ni	Zn	Ti	Pb	Sn
wt.%	7.5	0.15	0.03	0.03	0.60	0.03	0.05	0.20	0.03	. . .

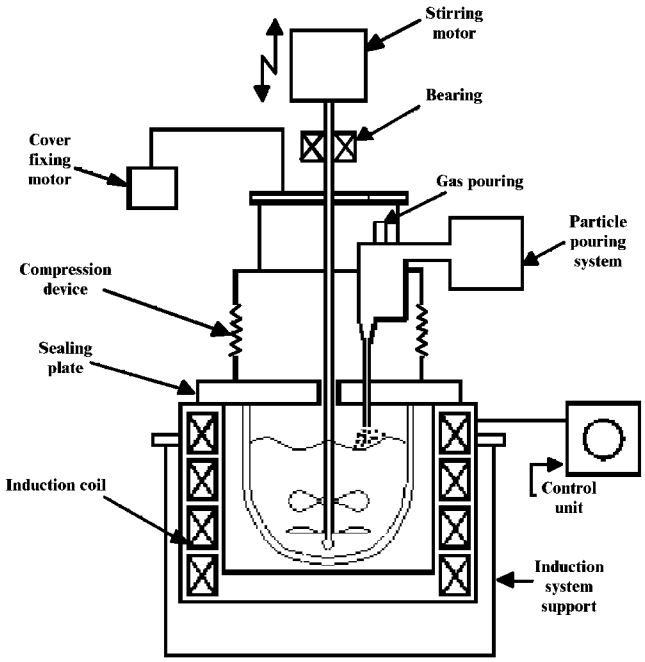

Fig. 1 Schematic diagram for fabrication of MMCs by using both mechanical stirring and electromagnetic stirring process

C.G. Kang, School of Mechanical Engineering, Engineering Research Center for Net Shape and Die Manufacturing (ERC/NSDM), Pusan National University, Pusan 609-735, Korea; and **S.W. Youn** and **P.K. Seo,** Department of Mechanical and Precision Engineering, Graduate School of Pusan National University, Pusan 609-735, Korea. Contact e-mail: cgkang@hyowon.pusan.ac.kr.

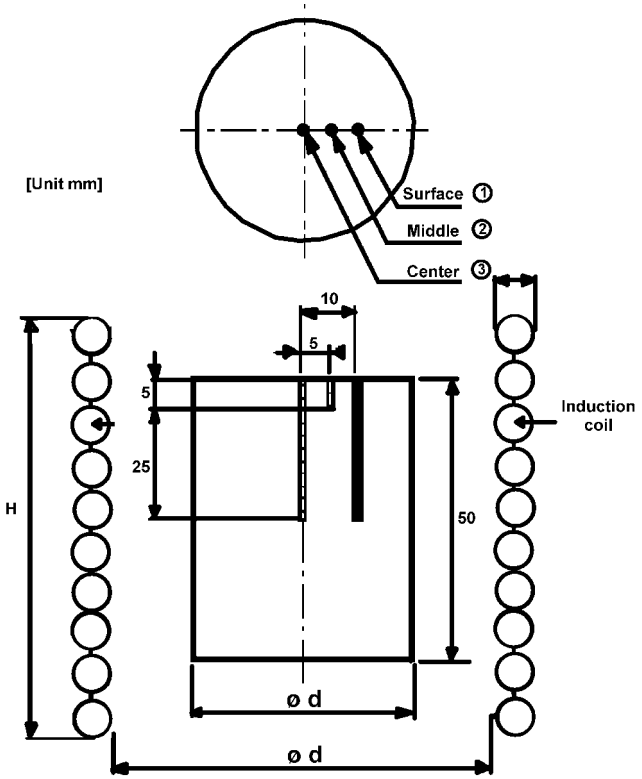

Fig. 2 Thermocouple positions for measuring temperature during the reheating process of metal matrix composites

Table 2 Chemical Composition of Silicon Carbide Particle

Content	SiC	C	SiO_2	Fe	PH (a)
wt.%	99.0	0.04	0.55	0.07	5.0 to 7.0

(a) PH: potential of hydrogen

Table 3 Recommended Air Gaps [1/2(D_i − d)] and Coil Wall Thickness (d_c) for Through-Heating Coils

Frequency	Air Grip [1/2(D_i = d)] (mm)	Coil Wall Thickness (d_c:m)
10 kHz	3	3.2
25 kHz	2	1.7

Table 4 Material Properties for Calculating the Composites Properties

Material	Parameter	Symbol	Unit	Value	Reference
A357	Thermal conductivity	k	W/mK	152	26
	Resistivity	ρ	μΩm	0.0421	
SiCp	Thermal conductivity	k	W/mK	110	26
	Resistivity	ρ	μΩm	0.1	

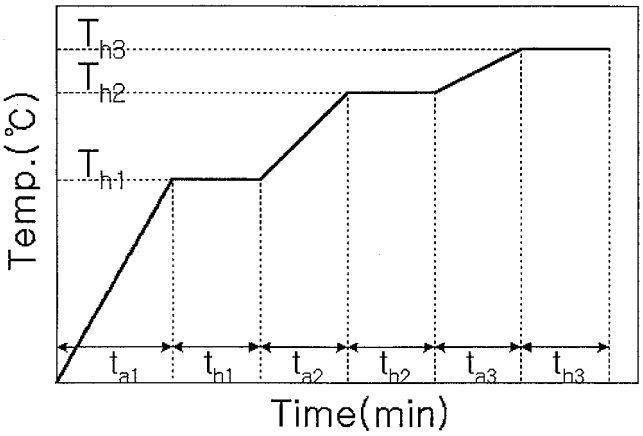

Fig. 3 Schematic illustration of reheating conditions to obtain semi-solid material in metal matrix composites

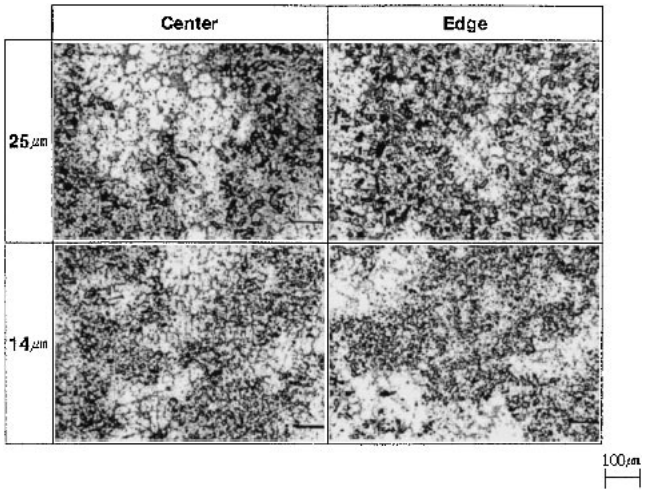

Fig. 4 Microstructure of metal matrix composites fabricated by the combined stirring process (595 °C, 15 vol.% and 600 rpm)

vary particle size. The PMMCs were tested before and after reheating using a tensile test with and without heat treatment. The combined process condition with mechanical and electromagnetic stirring for fabricating the PMMCs also is suggested. For the thixoforming of PMMCs, fabricated billets are reheated by using an induction-heating device. The present study focused on the influence of the dispersion state of the SiCp particles on the induction heating temperature and globular microstructure.

2. Experimental Procedure

2.1 Production of PMMC Billets

The matrix material used for the fabrication of PMMCs was an aluminum alloy, A357, fabricated by the electromagnetic stirring process and made by Pechiney (Voreppe, France). The chemical composition of the A357 is shown in Table 1. The silicon carbide particles used in these experiments were provided by Showa Denko Company (Japan), and the chemical composition and PH are shown in Table 2.

Table 5 Property Values to Calculate the Effective Coil Length of the Metal Matrix Composites with Billet Diameter 40 mm and Length 50 mm, f = 20 kHz, δ = 0.65 mm

Parameter	Symbol	Unit	Value	Reference
Maximum surface-center temperature difference	$\theta_s - \theta_c$	K	3	
Thermal conductivity	k_c	W/mK	147.8	
Idealized power density	P_s	kW/m^2	44.34	
Resistivity of PMMCs	ρ_c	$\mu\Omega$m	0.0478	
Magnetic constant	μ	H/m	$4\pi \times 10^7$	24
Angular frequency	ω	rad/s	$4 \times 10^4\pi$	
Finite current depth of penetration	δ_F	m	0.78×10^{-3}	
Actual power density	P_a	kW/m^2	47.67	
Thermal power	P_t	kW	0.256	
Production rate	P_r	Dimensionless	0.01 t/h	25
Thermal capacity	q	kW	25.64 h/t	
Minimum heated surface area	A_s	m^2	5.37×10^{-3}	
Billet diameter	d	mm	40	
Minimum heated length	l_w	mm	43	

Table 6 Designed Dimensions of the Induction Heating Device (f = 20 kHz, δ = 0.65 mm)

Volume Fraction (%)	Billet Diameter (d:mm)	Coil Inner Diameter (D_i:mm)	Min. Heating Length (l_w:mm)	Effective Coil Length (H:mm)
5 to 15	40	44.6	42 to 44	69 to 119

Table 7 Reheating Conditions of Metal Matrix Composites for Thixoforming (SiCp 25 μm)

Vol.%	Test Specimen (mm)	Heating Time t_a (mm)			Heating Temp. T_h (°)			Holding Time T_h (mm)		
		t_{a1}	t_{a2}	t_{a3}	T_{h1}	T_{h2}	T_{h3}	t_{h1}	t_{h2}	t_{h3}
0	$d \times l = 40 \times 50$	3	2	1	451	576	582	1	1	2
5		3	1	1	501	575	580	1	2	1
10		3	1	1	501	575	582	1	2	1
15		3	1	1	501	575	593	1	2	2

Figure 1 shows a schematic diagram of the composite stirrer designed and manufactured to obtain the homogeneous stirring. Mixing of SiC particles with the molten aluminum alloy A357 was performed in a clay graphite crucible placed inside a high-frequency furnace. The particles had an average size of 14 μm and 25 μm and were mixed into the melt with an impeller, manufactured from graphite, that was driven by a variable DC motor.

The characteristics of the stirring device are as follows. The impeller shaft was made of SUS 316. The impeller was lowered into the melt and attached to the motor shaft. The clearance of the impeller from the bottom of the crucible was approximately 10 mm, the melt depth being approximately 50 mm. The stirrer was turned on and set to the predetermined speed. The top of the high-frequency furnace was covered with an adiabatic board. Thermocouples were inserted into the molten alloy and the furnace to measure their exact temperatures.

Table 8 Reheating Conditions of Metal Matrix Composites for Thixoforming (SiCp 14 μm)

Vol.%	Test Specimen (mm)	Heating Time t_a (mm)			Heating Temp. T_h (°)			Holding Time T_h (mm)		
		t_{a1}	t_{a2}	t_{a3}	T_{h1}	T_{h2}	T_{h3}	t_{h1}	t_{h2}	t_{h3}
0	$d \times l = 40 \times 50$	3	2	1	451	576	582	1	1	2
5		3	1	1	501	575	582	1	2	1
10		3	1	1	501	575	583	1	2	1
15		3	1	1	501	575	595	1	2	2

The proper amount (750 to 780 g) of the matrix washed with acetone was charged into the graphite crucible placed inside a high-frequency furnace. The matrix was heated up to the molten metal state (over 630 °C). After oxide films generated by the contact with atmosphere were removed, the cover fixing motor was driven to make the cover contact with the crucible. After driving the stirring impeller, the melted matrix was held and stirred at 595 °C for 1 min. The SiC particles of 10 g per unit min were added uniformly for approximately 15 min. The stirring impeller was coated with a fiberfrax coating cement (Carborundum Company, Amhurst, NY) and preheated up to 500 °C to prevent a rapid decrease in temperature by the contact with the matrix. After the particle addition, the impeller was driven for 15 min, and the melted PMMCs were poured in the preheated graphite mold. The poured melt was cooled in the mold for 1 min and then was water-quenched.

The fabricated PMMC billet diameter was 40 mm, and the length was 180 to 200 mm. To reheat the billet, the machined billet length was 50 mm and diameter was 40 mm without machining.

2.2 Fundamentals of Inductive Coil Design for the Uniform Reheating of PMMCs

Induction heating is due to eddy current heating on the surface and requires the influence of conduction to heat the center of the PMMC billet. In the case of heating the PMMC billet by using an induction heater, because the reheating conditions are different due to the variation of PMMCs and billet size, the inductive coil design and construction of a quantitative

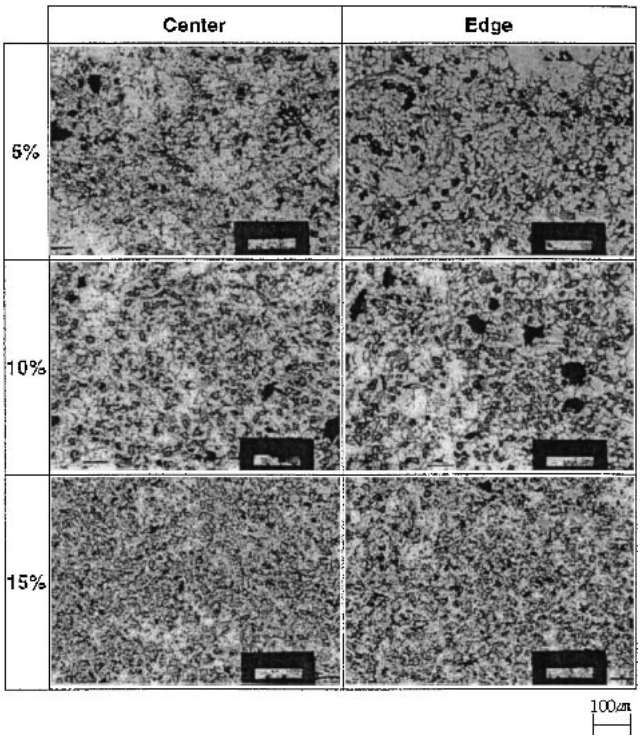

Fig. 5 Microstructure of metal matrix composites fabricated by the combined stirring process (matrix temperature 595 °C, a particle size of 25 μm, and stirring speed of 1200 rpm)

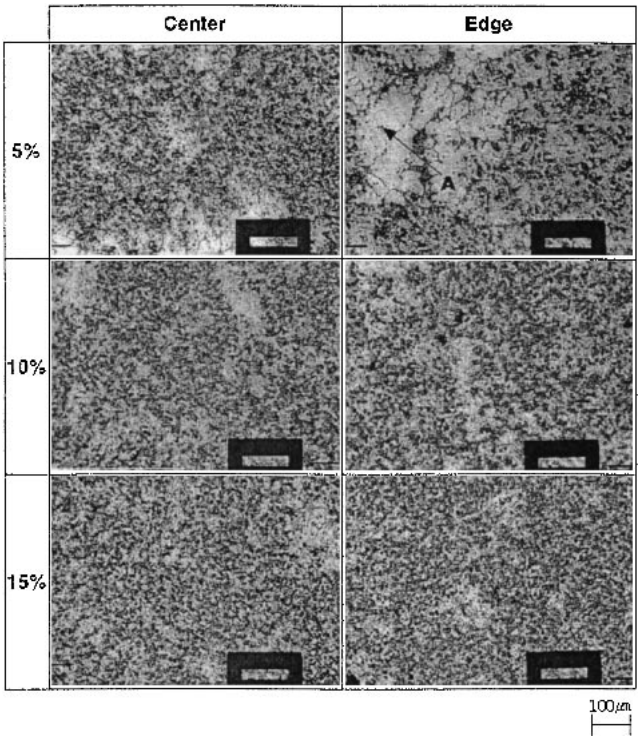

Fig. 6 Microstructure of metal matrix composites fabricated by the combined stirring process (matrix temperature 595 °C, a particle size of 14 μm, and stirring speed of 1200 rpm)

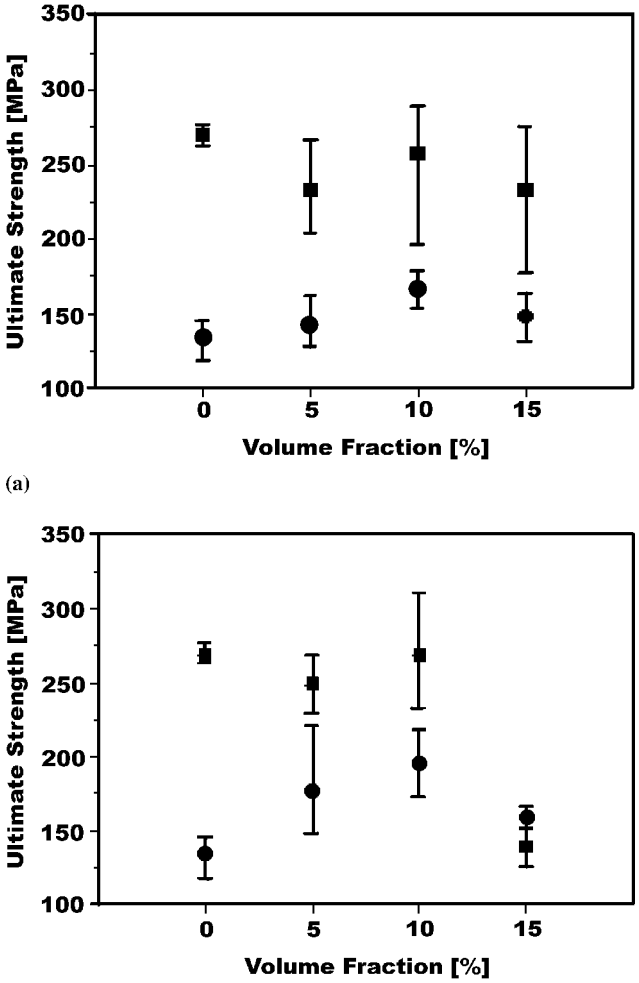

Fig. 7 Ultimate tensile strength distribution of metal matrix composites fabricated by the combined stirring process (●, before heat treatment, ■ after heat treatment). **(a)** particle size of 25 μm; **(b)** particle size of 14 μm

reheating database for the thixoforming of PMMCs are very important.[19-22]

In commercial induction heating systems, including the induction heating of aluminum billets with reinforcement, the induced heat is normally not equally distributed over the length of the PMMC billet. This effect is called "skin effect." Because of the skin effect, approximately 86% of the power is concentrated in a surface layer of the inductively heated billet. This layer is called the current depth of penetration. The degree of skin effect depends on the frequency and material properties, such as electrical resistivity and magnetic permeability of the PMMC billet.

Non-uniformity of the heating profile at the coil and billets ends of composites is related to the distortion of the electromagnetic field in those areas. This distortion is called the electromagnetic end effect. In general, the electromagnetic end effect is one of the most complicated problems in induction heating. This effect can result in either the overheating or underheating of the billet ends. Therefore, the desired temperature distribution may be obtained only with a particular coil dimension.

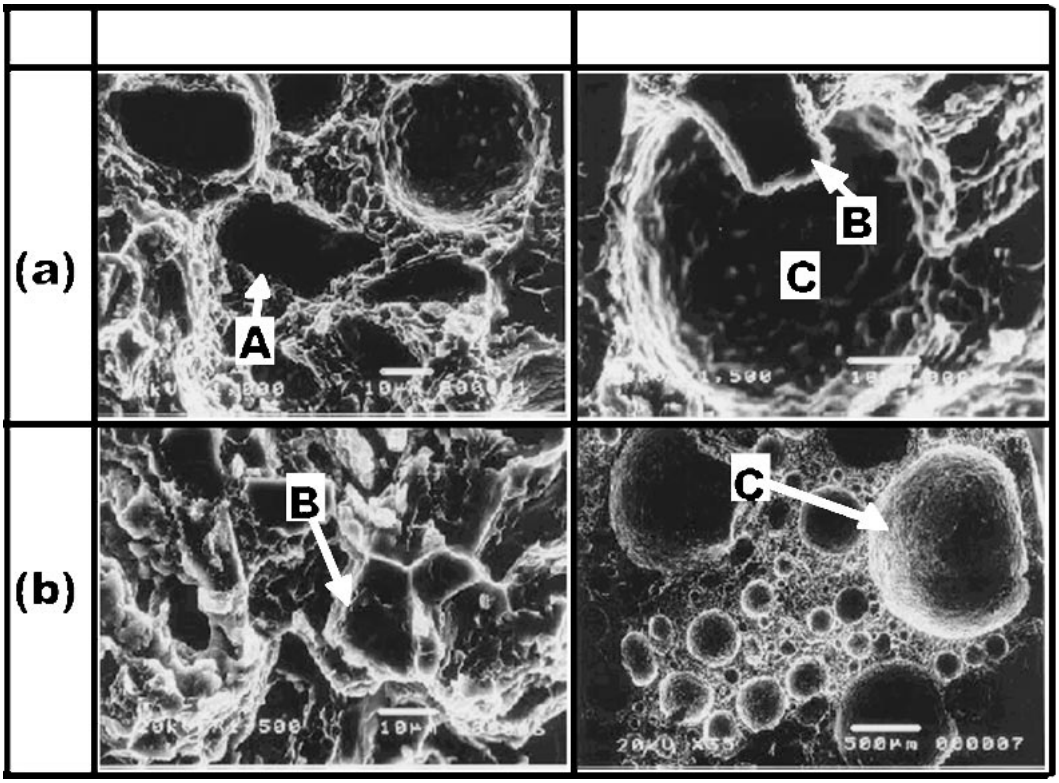

Fig. 8 SEM fractograph of A357/SiCp tensile specimen **(a)** SiCp 25 μm **(b)** SiCp 14 μm

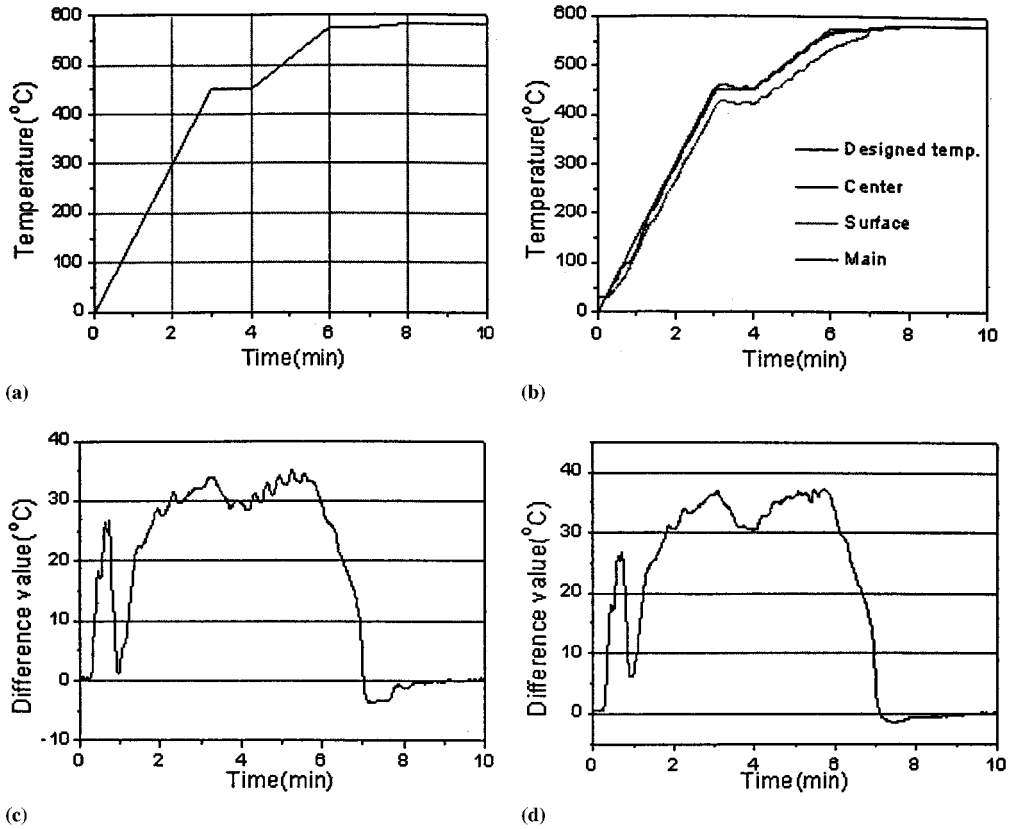

Fig. 9 Set temperature and measured temperature-time curves during the reheating process of A357 billet. **(a)** set temperature profile; **(b)** temperature profile; **(c)** difference value between center and surface; **(d)** difference value between main and surface

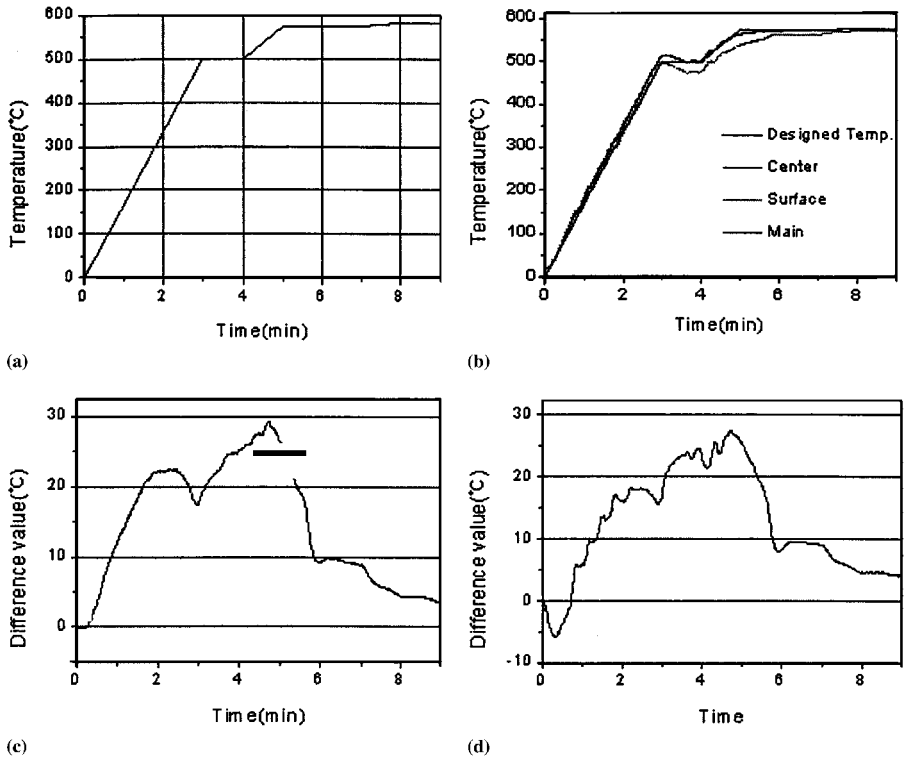

Fig. 10 Set temperature and measured temperature-time curves during the reheating process of metal matrix composites fabricated by the combined stirring process (a particle size of 25 μm and 5 vol.%)

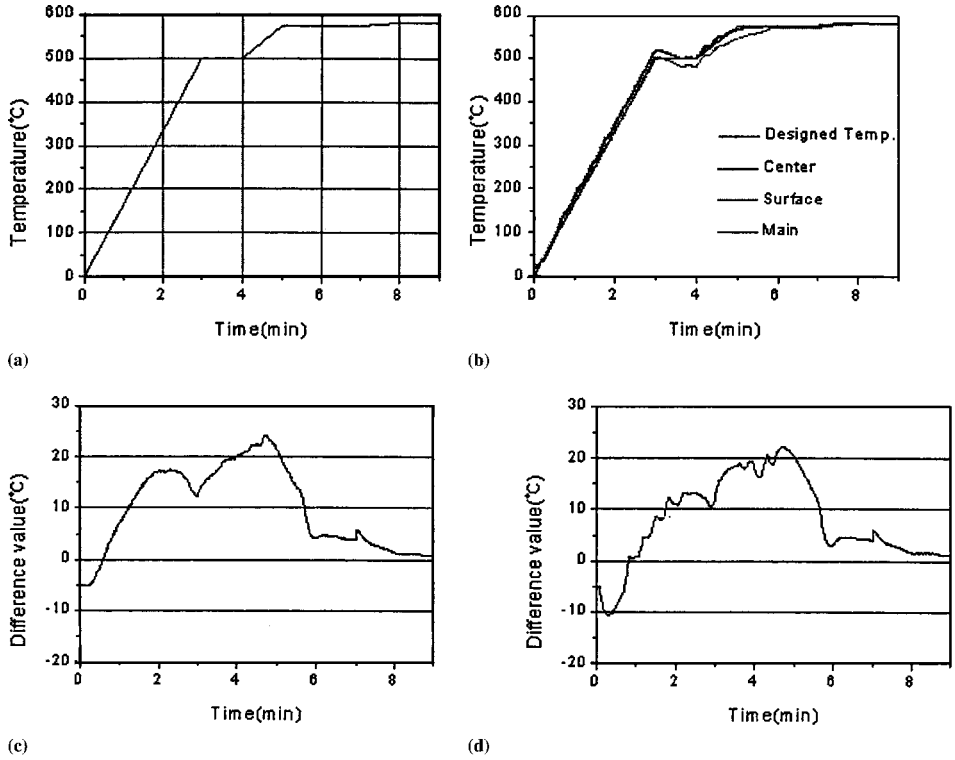

Fig. 11 Set temperature and measured temperature-time curves during the reheating process of metal matrix composites fabricated by the combined stirring process (a particle size of 25 μm and 10 vol.%)

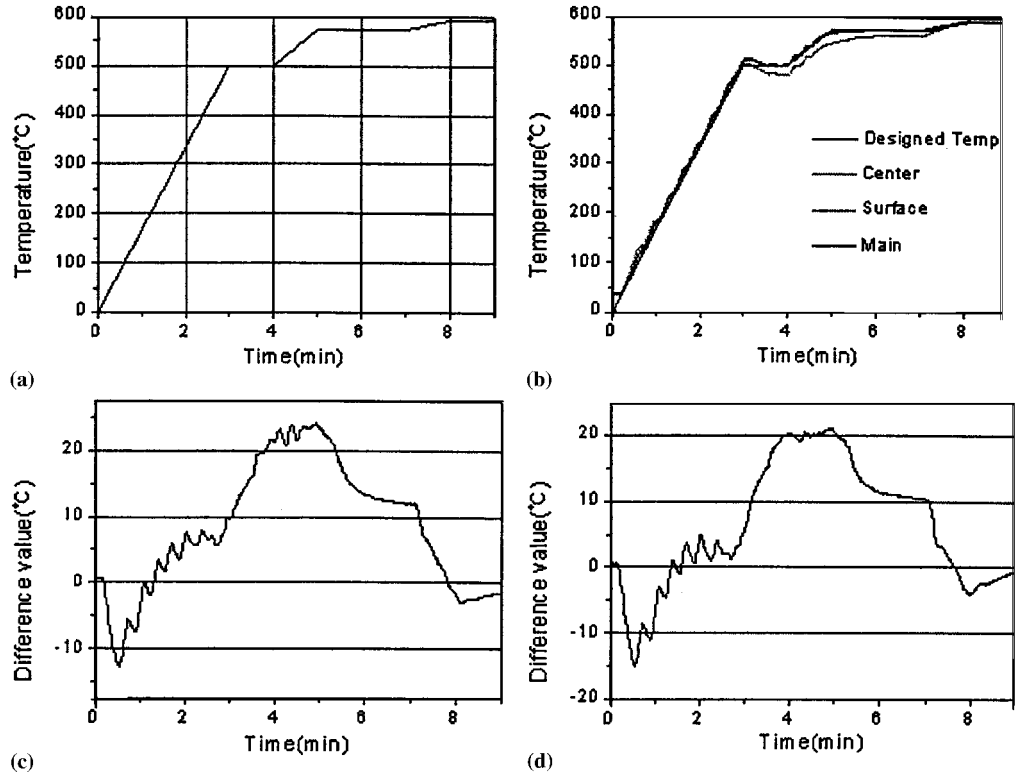

Fig. 12 Set temperature and measured temperature-time curves during the reheating process of metal matrix composites fabricated by the combined stirring process (a particle size of 25 μm and 15 vol.%)

For a real system consisting of coil and the PMMC billet, the induced heat over the length of the PMMC billet generally is not equally distributed and, consequently, there is a non-uniform temperature distribution. Therefore, an important point for coil design is to verify the correct relationship between coil length and billet length.[1,19,20,23]

To uniformly reheat PMMCs in this present work, the effective coil length H and coil inner diameter, D_i, of the induction heating device were designed, as shown in Fig. 2. To consider the main surface power loss in induction heating, the idealized power density (P_s) must be represented as the actual power density (P_a), which is modified to allow for the ratio ($d/2\delta_F$) of a finite current depth of penetration (δ_F) of material and billet diameter (d).

$$\delta_F = \sqrt{\frac{2\rho_c}{\mu\omega}} \quad \text{(Eq 1)}$$

$$P_a = \frac{P_s(\theta_s - \theta_c)_{idealized}}{\theta_s - \theta_c} = \frac{4.3k_c(\theta_s - \theta_c)}{d} \quad \text{(Eq 2)}$$

In Eq 2,

$$\frac{\theta_s - \theta_c}{(\theta_s - \theta_c)_{idealized}} = k$$

can be obtained from the variation curves of temperature in a cylinder with finite current depth of penetration,[24] where P_c, μ,W,K, and $\theta_s - \theta_c$ are the resistivity of PMMCs, the magnetic constant, the angular frequency, the thermal conductivity, and the maximum surface-center temperature difference, respectively.

If a diameter of 40 mm and a length of 50 mm is assumed to be reheated to 592 °C, 596 °C, and 598 °C, because, by Stansel's data (in the case of a temperature rise to 510 °C, the thermal capacity of q = 145 kW h/t and the production rate of P_r = 0.01 t/h),[25] and linear interpolation, the thermal capacity q, and the production rate P_r are calculated, and the minimum heated surface area A_s and the minimum heated length l_w can be determined as follows:

$$A_s = \frac{P_t}{P_a} = \frac{P_r \times q}{P_a} \quad \text{(Eq 3)}$$

$$l_w = \frac{A_s}{\pi d} \quad \text{(Eq 4)}$$

To determine the coil inner diameter D_i and effective coil length H, recommended air gaps [1/2 ($D_i - d$)] for through-heating coils and property values to calculate the effective coil length are shown in Tables 3-5, respectively. The property values of PMMCs with volume fraction (V_f) are calculated by Eq 5 and 6:

$$k_c = (1 - V_f)\, k_m + V_f k_r \quad \text{(Eq 5)}$$

$$\rho_c = (1 - V_f)\, \rho_m + V_f \rho_r \quad \text{(Eq 6)}$$

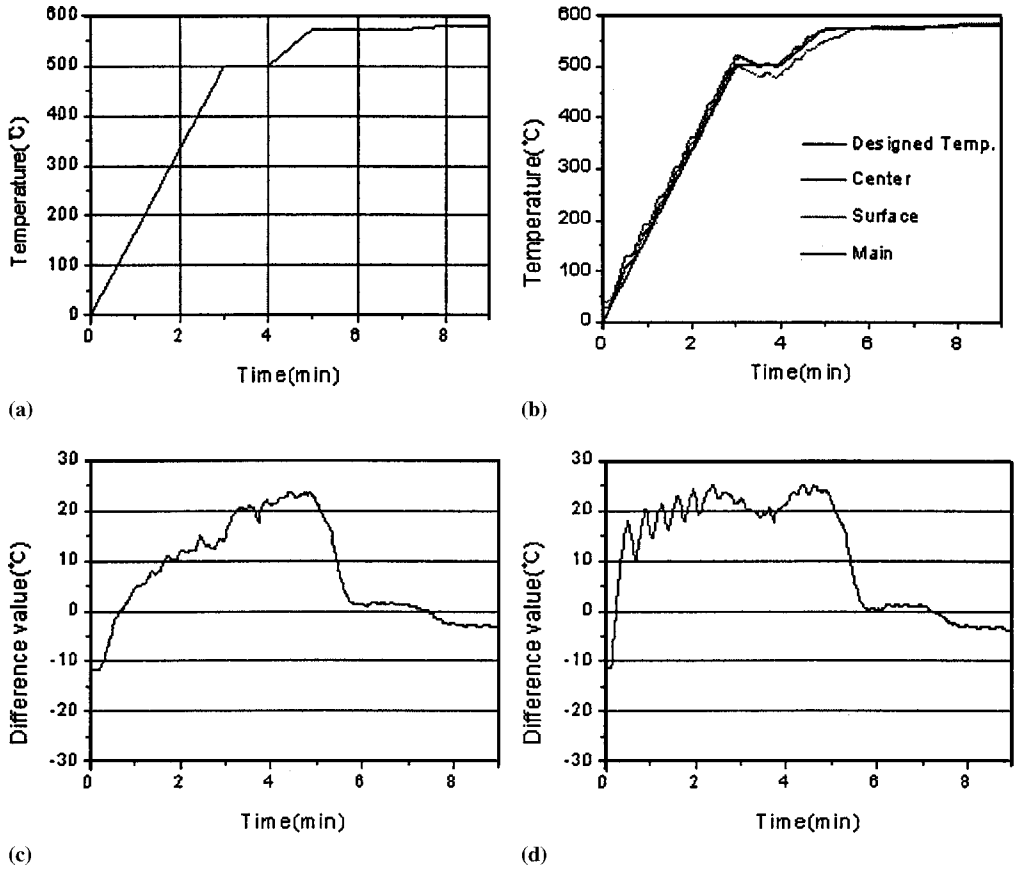

Fig. 13 Set temperature and measured temperature-time curves during the reheating process of metal matrix composites fabricated by the combined stirring process (a particle size of 14 μm and 5 vol.%)

where ρ_c and k_c are density and thermal conductivity of composites, respectively, k_m and k_r are thermal conductivity of matrix and reinforcement, and ρ_m and ρ_r are the density of matrix and reinforcement, respectively.

By using linear interpolation with Table 3, the coil inner diameter D_i is calculated, and from the result of Eq 4, the effective coil length H can be calculated by Eq 7:

$$H = l_w + (25 \text{ to } 75) \quad \text{(Eq 7)}$$

Therefore, from the above considerations, the coil dimensions for the PMMCs reheating for thixoforming are proposed as in Table 6, and the experiments of reheating are performed by using those dimensions.

2.3 Reheating PMMC Billets

For the thixoforming process, the reheating process of PMMCs is very important; the process is not only necessary to perform the desired semi-solid material billet state but also to control the microstructure of the PMMC billet.

PMMC billets fabricated by combined stirring were machined to reheating process, at which point the diameter was 40 mm and the length was 50 mm. The reheating experiments were executed using an induction heating system with a capacity of 20 kW. The heating coil of the induction heating system was made by with a coil diameter (D_o) of 80 mm and a coil length (H) of 100 mm. Thermocouple holes to measure the temperature accurately were machined to a 2 mm diameter 10 mm from the surface of the billet and the position of billet depth 30 mm, as shown in Fig. 2. To accurately control the temperature of the PMMCs, K-type CA thermocouples of 1.6 mm were inserted into the billet. The thermocouples were calibrated using 100 °C water. The accuracy of thermocouples is approximately 0.2%. A data logger TDS-302 (Tokyo Sokki Kenkyuio Co., Ltd., Tokyo) was used to receive the data, and the heating temperature was set to the data as a thermocouple position "main" in Fig. 2. In this study, the reheating temperature of PMMCs was determined from the relationship of the matrix temperature and solid fraction, including reinforcement.[27]

The reheating experiments were carried out for the conditions in Tables 7 and 8. The meanings of the symbols used in Tables 7 and 8 are the same as those shown in Fig. 3.

3. Experimental Results and Discussion

3.1 Dispersion State of PMMCs

The most important point in the fabrication process of PMMCs is the uniform dispersion of the reinforcements. The

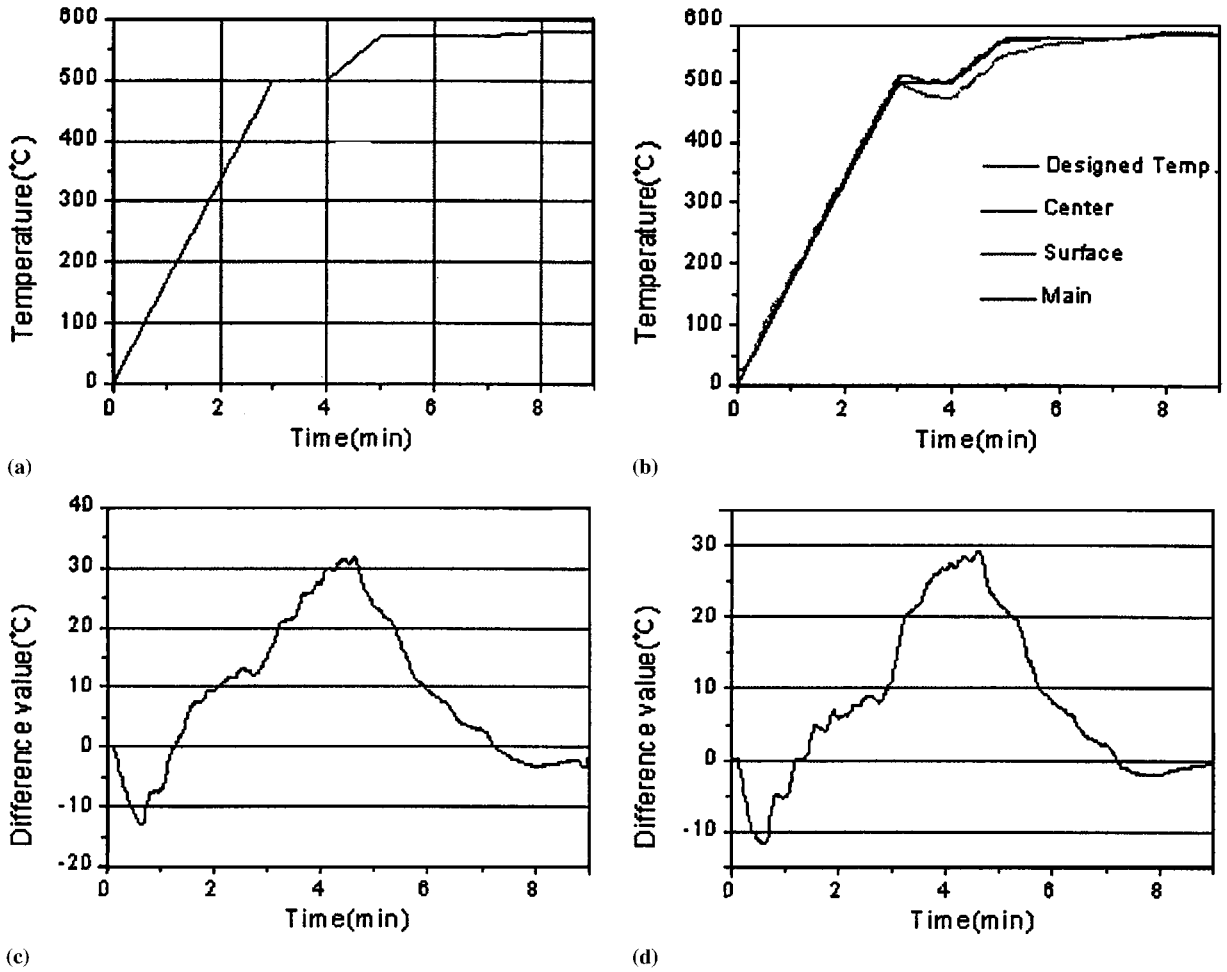

Fig. 14 Set temperature and measured temperature-time curves during the reheating process of metal matrix composites fabricated by the combined stirring process (a particle size of 14 μm and 10 vol.%)

interaction parameters between SiCp and a growing solid/liquid interface are the alloying elements and the cooling rate. Particle capture or rejection is governed mainly by the Si content in the matrix. In hypoeutectic alloy such as A357 where the Al dendrites solidify first, the particle distribution after solidification is dependent on the cooling rate.[28]

In these experiments, the temperature of the matrix-particulate mixture was maintained at 595 °C. The fabrication conditions were set to obtain uniform dispersion for various stirring speeds.

Figure 4 shows the optical micrographs of obtained at a stirring speed of 600 rpm with SiCp (15 vol.%). As shown in Fig. 4, agglomerated SiCp particles were observed. At low stirring speeds, the semisolid stirring process had no influence on the uniformity of dispersion of the reinforcements.

Figures 5 and 6 present micrographs showing the dispersion state for an increased stirring speed of 1200 rpm. As shown in Fig. 5, in the case of the particle size of 25 μm, reasonably uniform dispersion was obtained, independent of volume fractions. In the case of the particle size of 14 μm, the dispersion state of the reinforcements was not more uniform than that of the particle size of 25 μm. This may be explained by the particles rejected by the solid/liquid interface. As a result of this phenomenon, the particles segregated to the inter-dendritic region.

3.2 Mechanical Properties and Microstructure of Fabricated PMMCs

The T6 heat treatment conditions used for fabricated PMMCs were as follows. Specimens were solution heat-treated at 530 °C for 2 h and quenched in water. Aging was performed at 175 ° for 8 h, and the specimens were air-cooled to room temperature. Tensile strength was measured on machined specimens using an MTS machine with a maximum load of 25 tons. Figure 7 shows the ultimate strength for composites test specimen with heat treatment conditions (with and without T6 heat treatment). The tensile strength increased as volume fractions increased. This phenomenon was independent of the size of SiCp particles. However, the tensile strength decreased at a volume fraction of 15%. On a tensile test, a maximum tensile strength was measured at the volume fraction of 10%. This is because the bonding force between the matrix and the particles in the region of clusters (position "A" in Fig. 8) is weak. Figure 8 shows the SEM fractographs of A357/SiCp tensile specimen for two different particle sizes of 25 μm and 14 μm. The preceding results show the weakness of the bonding force at the interface between the matrix and the SiCp particles. This may be explained by many porosities (position "C" in Fig. 8) generated by air entrance in pouring the melt. Therefore,

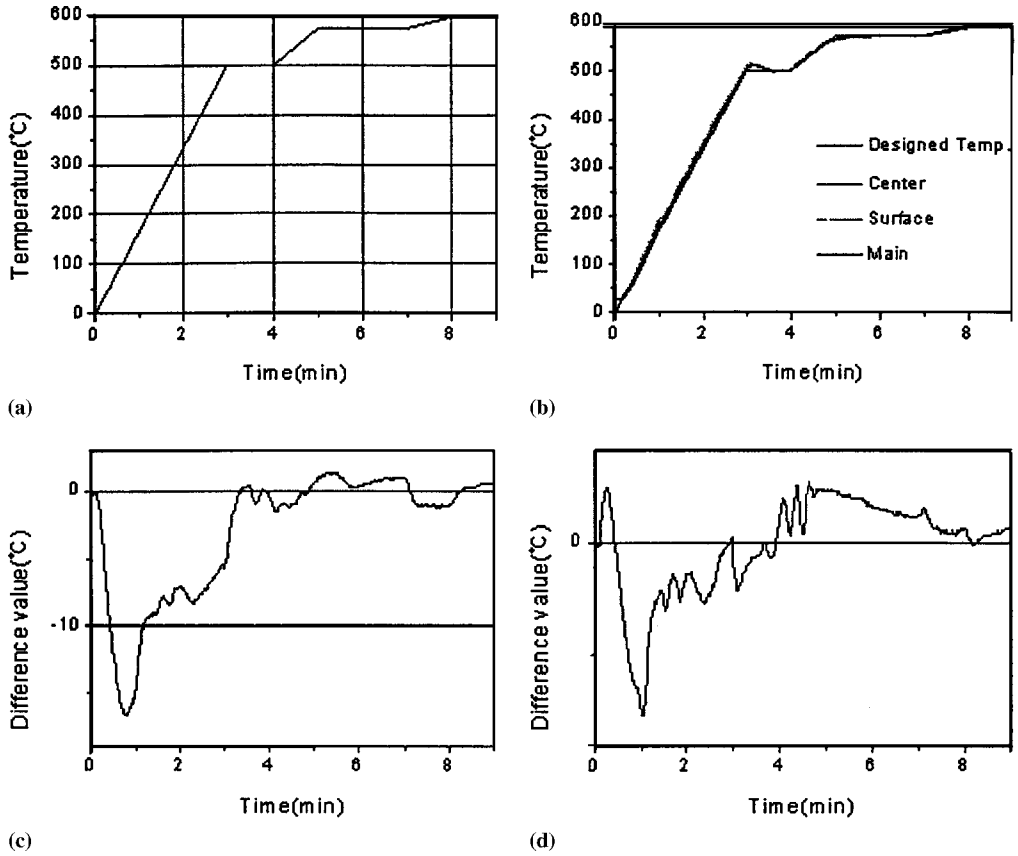

Fig. 15 Set temperature and measured temperature-time curves during the reheating process of metal matrix composites fabricated by the combined stirring process (a particle size of 14 μm and 15 vol.%)

through the use of air vent, the interfacial bonding force was considered to be improved.

3.3 Reheating Experiments

The microstructure of PMMCs after reheating must be a globular one. Furthermore, when the PMMCs are fed from the reheating device to the die, the shape of the PMMCs must be maintained. Therefore, the volume fraction of the reinforcement and SiCp particle size were considered as parameters of the reheating experiment to obtain the globular microstructure and a small temperature gradient. To determine the heating temperature of the PMMCs, the solid fraction of A357/SiCp is used as a reference.[27]

Figure 9 represents the set temperature and measured temperature-time curves during the reheating process of unreinforced A357 billet. In this case, the A357 billets reach the set temperature with a small temperature difference (about 2 °C).

Figures 10-15 show the set temperature and measured temperature-time curves during the reheating process of metal matrix composites fabricated for the variation of volume fractions. In the case of 15 vol.%, the reheating temperature of PMMCs was approximately 13 °C higher than unreinforced A357. The effects of dispersion state of the reinforcements were observed remarkably during the reheating process of PMMCs. Moreover, in the case that the SiCp particle dispersed uniformly, the total reheating time of the PMMCs was reduced and the reheating temperature of the final step was low.

Figure 16 presents the reheating conditions of PMMCs according to the dispersion state. In the case that the reinforcement dispersed uniformly, the set temperature of the final reheating step was approximately 11 °C lower than that of the non-uniformly dispersed reinforcements and the total reheating temperature of the final step was also approximately 3 min shorter than that of the non-uniformly dispersed state.

Figures 17 and 18 show the microstructures after the reheating process of metal matrix composites fabricated by the semi-solid stirring process. Uniform globular microstructures with a grain size of 100 μm as well as uniformly dispersed reinforcements were observed at all positions.

From the proceeding results, it was found that the total reheating time to reach the desired temperature in reheating process of PMMCs depends on the dispersion state of the reinforcements in fabricated composites billet. At the present time, research on obtaining a more uniform dispersion state of the particles by the control of solid fractions is being performed. Figure 19(a) and (b) shows the ultimate strength after reheating process. As shown in Fig. 19(a) and (b), the ultimate strength is higher than that of Fig. 7 with composites without reheating. After reheating of composites, it is cause that the globularization microstructure in matrix alloy is obtained after reheating of composite, as shown in Fig. 16 and 17.

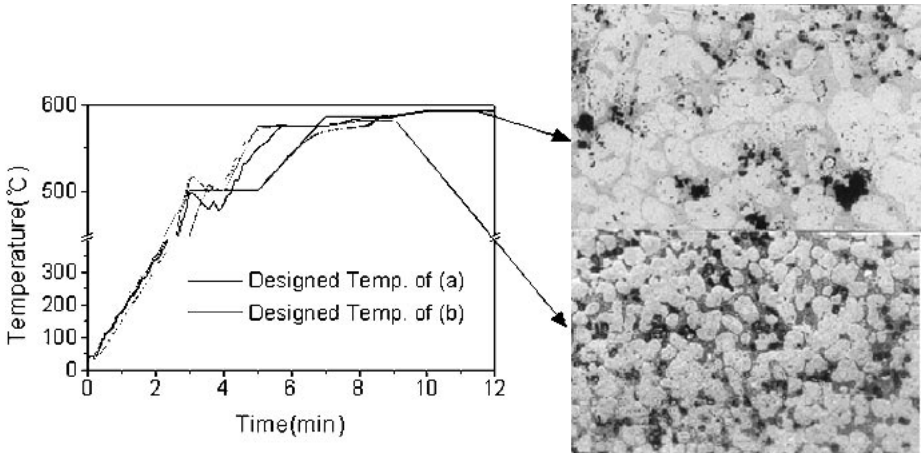

Fig. 16 Temperature profile during the reheating process and microstructure of PMMCs after reheating process

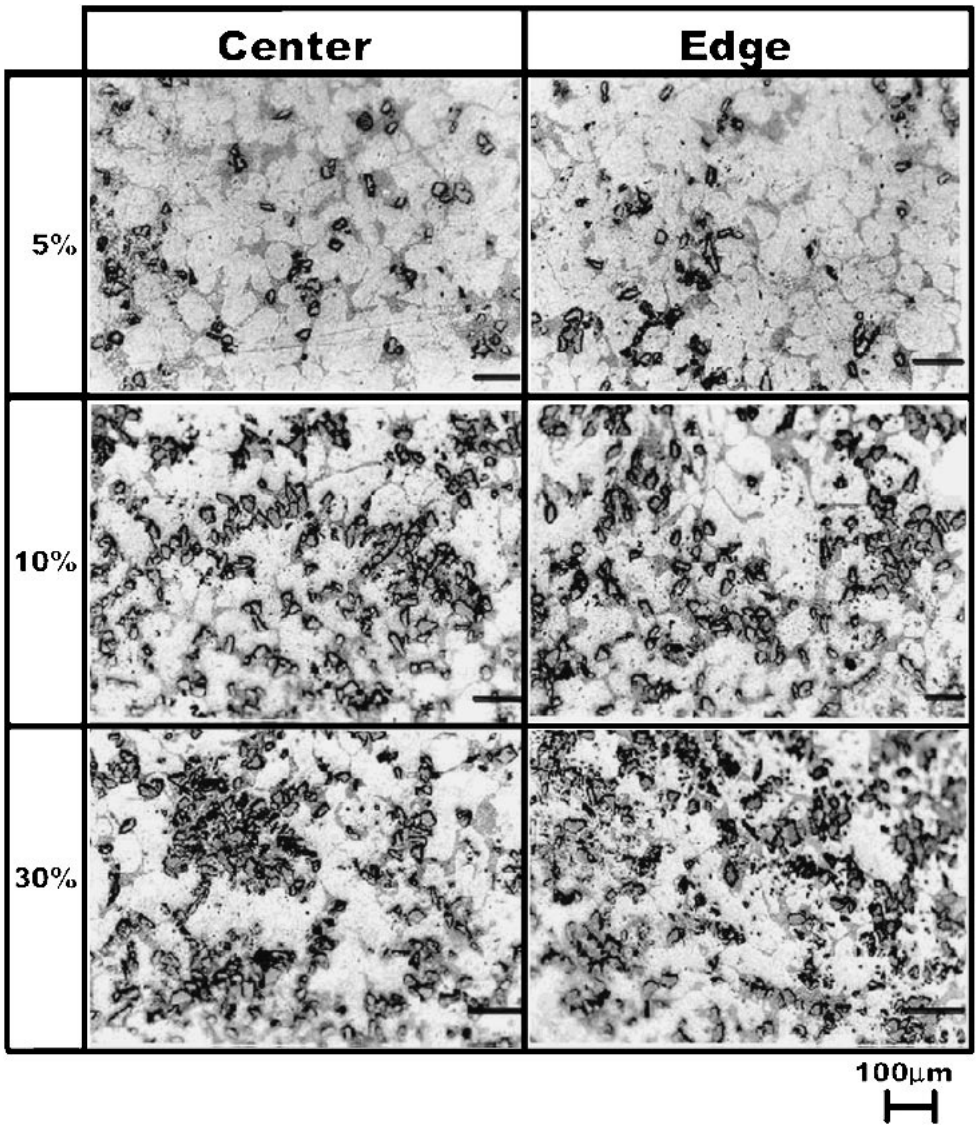

Fig. 17 Microstructure after the reheating process of metal matrix composites fabricated by the combined stirring process (a particle size of 25 μm)

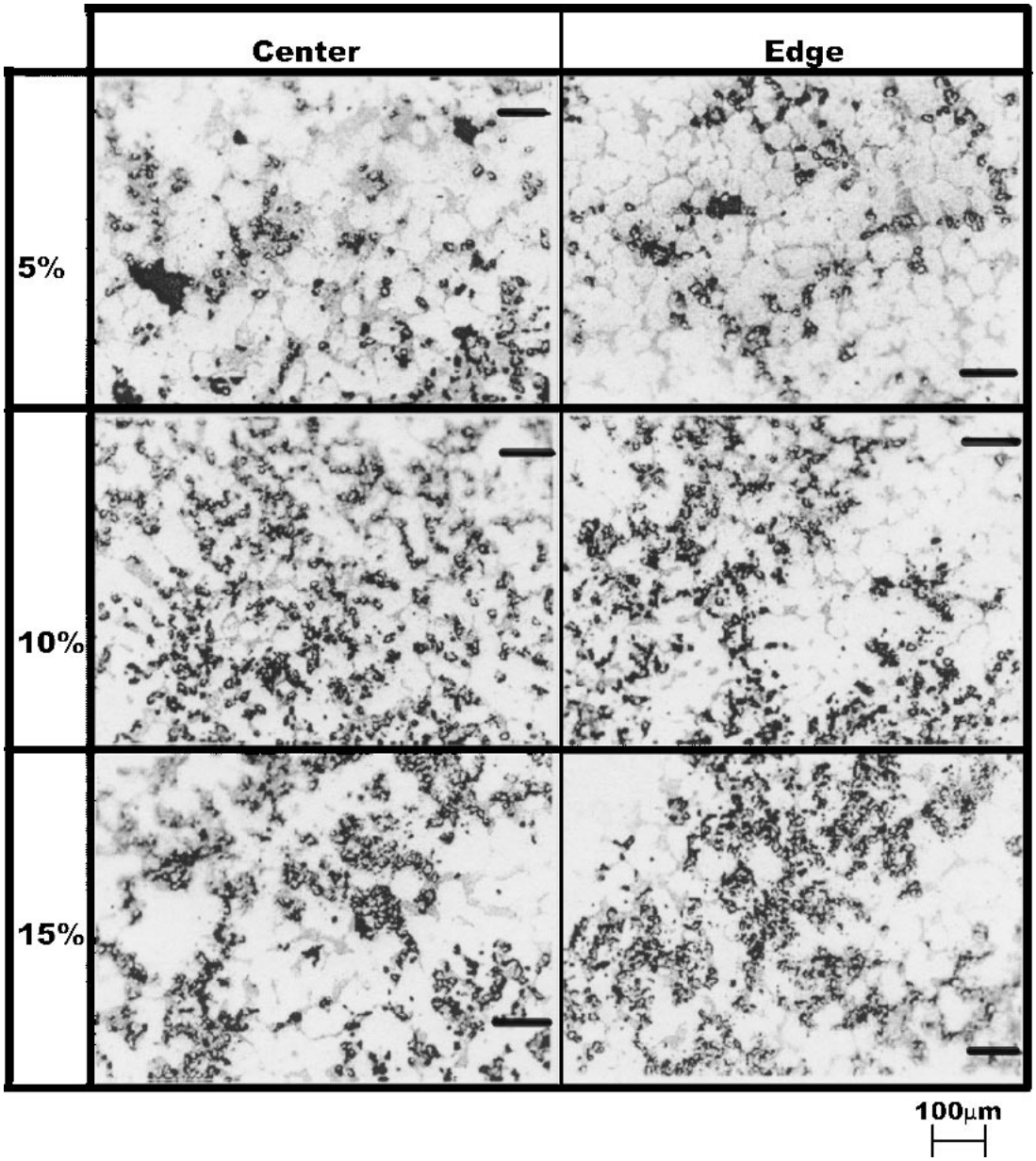

Fig. 18 Microstructure after the reheating process of metal matrix composites fabricated by the combined stirring process (a particle size of 14 μm)

4. Conclusions

Through the fabrication process of PMMCs using the compocasting method and the reheating experiments for thixoforming, the particular conclusions are summarized. The effective coil dimensions in the reheating process for thixoforming metal matrix composites were proposed by the analysis method to avoid eddy current and temperature difference in an entire cross-sectional area. In the case of the particle size of 25 μm, reasonably uniform dispersion was obtained independent of volume fractions. In the case of the particle size of 14 μm, the dispersion state of the reinforcements was not more uniform than that of the particle size of 25 μm. The tensile strength increased as volume fractions increased. However, the tensile strength decreased at a volume fraction of 15%. This is because the bonding force between the matrix and the particles in the region of clusters is weak.

The SEM fractographs of A357/SiCp tensile specimen show the weakness of the bonding force at the interface between the matrix and the SiCp particles. This may be explained by the multiple porosities generated by air entering while pouring the melt. Therefore, through the use of an air vent, the interfacial bonding force was improved. In the case that the reinforcement dispersed uniformly, the set temperature of the final reheating step was approximately 11 °C lower than that of the non-uniformly dispersed reinforcements and the total reheating

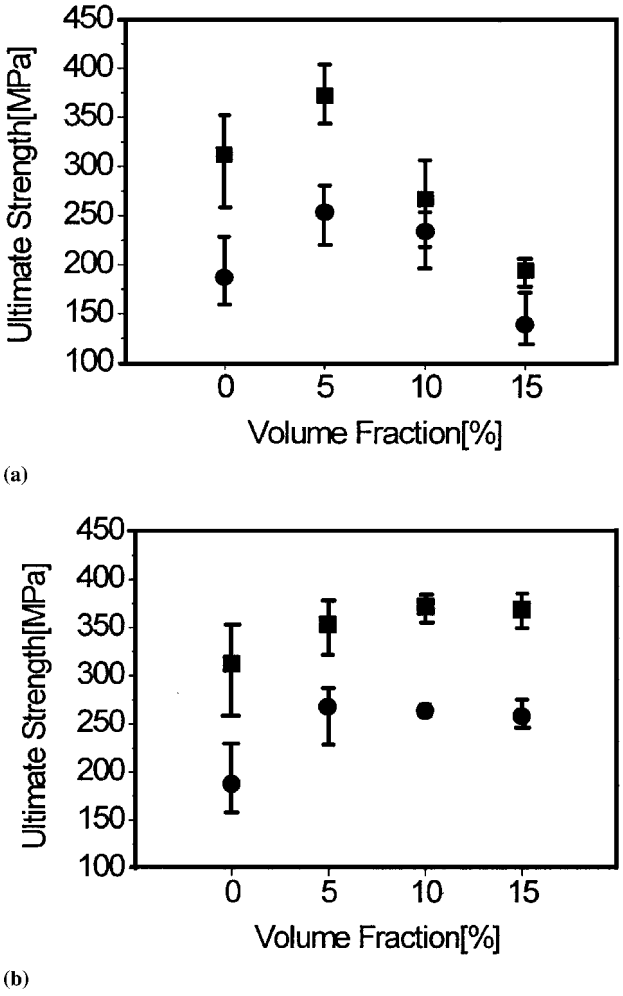

Fig. 19 Ultimate strength of metal matrix composites after reheating process. (● before heat treatment; ■ after heat treatment)

temperature of the final step was also approximately 3 min shorter than that of the non-uniformly dispersed state. Through the microstructure observation after the reheating process of metal matrix composites fabricated by the semisolid stirring process, uniform globular microstructures with a grain size of 100 μm as well as uniformly dispersed reinforcements were observed at all positions.

In conclusion, it was found that the most important factors regarding the reheating process of PMMCs are heating time, heating temperature, and holding time for each step during induction heating of composites fabricated using mechanical stirring and electromagnetic stirring process.

Acknowledgments

This work has been supported by the Engineering Research Center for Net Shape and Die Manufacturing (ERC/NSDM), which is financed jointly by the Korea Science and Engineering Foundation (KOSEF). The financial assistance of the ERC/NSDM and KOSEF is gratefully acknowledged.

References

1. C.G. Kang and H.K. Jung: "Semisolid Forming Process—Numerical Simulation and Experimental Study," *Metall. Mater. Trans. B,* 2001, *32B*(2), pp. 363-72.
2. C.G. Kang and H.K. Jung: "A Study on Solutions for Avoiding Liquid Segregation Phenomena in Thixoforming Process: Part I. Constitutive Modeling and Finite Element Method Simulations for Die Design," *Metall. Mater. Trans. B,* 2001, *32B*(1), pp. 119-27.
3. C.G. Kang and H.K. Jung: "A Study on Solutions for Avoiding Liquid Segregation Phenomena in Thixoforming Process: Part II," *Metall. Mater. Trans. B,* 2001, *32B*(1), pp. 129-36.
4. C.G. Kang and H.K. Jung: "A Study on a Thixoforming Process Using the Thixotropic Behavior of an Aluminum Alloy with an Equiaxed Microstructure," *J. Mater. Eng. Performance,* 2000, *9*(5), pp. 530-05.
5. H.K. Jung, P.K. Seo, and C.G. Kang: "Microstructural Characteristics and Mechanical Properties of Hypo-Eutectic and Hyper-Eutectic Al-Si Alloys in the Semi-solid Forming Process," *J. Mater. Processing Technol.,* 2001, *113*, pp. 568-73.
6. H.K. Jung and C.G. Kang: "Effect of Alloying Element on the Mechanical Behavior and Superficial Defects in Thixoforged Components of Al-Si Alloys," *Key Eng. Mater.,* 2000, *177-180*, pp. 565-70.
7. A. Zavaliangos: "Modeling of the Mechanical Behavior of Semisolid Metallic Alloys at High Volume Fractions of Solid," *Int. J. Mech. Sci.,* 1998, *40*(10), pp. 1029-41.
8. P. Giordano, F. Boero, and G. Chiarmetta: "Thixoformed Space-Frames for Series Vehicles: Study, Development and Applications," *Proc. 6th Int. Conf. on Semi-Solid Processing of Alloys and Composites (SSM2000),* Turin, 2000, M. Rosso and G. Chiarmetta, ed., Unione Industriale di Torino, Turin, Italy, 2000, pp. 29-34.
9. E. Nussbaum: "Semi-solid Forming of Aluminum and Magnesium," *Light Met. Age,* 1996, June, pp. 6-22.
10. S.P. Midson, R.B. Minkler, and H.G. Brucher: "Gating of Semi-Solid Aluminium Castings," *Proc. 6th Int. Conf. on Semi-Solid Processing of Alloys and Composites (SSM2000),* Turin, 2000, M. Rosso and G. Chiarmetta, ed., Unione Industriale di Torino, Turin, Italy, 2000, pp. 67-71.
11. E. Tzimas and A. Zavaliangos: "Mechanical Behavior of Alloys with Equiaxed Microstructure in the Semi-solid State at High Solid Content," *Acta Mater.,* 1999, *47*(2), pp. 517-28.
12. I.A. Ibrahim, F.A. Mohamed, and E.J. Lavernia: "Particulate Reinforced Metal Matrix Composites—A Review," *J. Mater. Sci.,* 1991, *26*, pp. 1137-56.
13. S. Watanabe, K. Saithoh, and S. Okaniwa: "Extrudability of Discontinuous Aluminium Alloy Composite Billets," *J. Japan Inst. Light Met.,* 1990, *40*(4), pp. 278-84.
14. T. Hikosaka: "Effect of Thermal Cycling on the Properties of Aluminum Alloy-Alumina Short Fiber Composites Hot Extruded," *J. Japan Foundrymen's Soc.,* 1994, *66*(6), pp. 424-29.
15. G.A. Rozak and J.J. Lewandowski: "Effects of Casting Conditions, and Deformation Processing on A356 Aluminium and A356-20vol% SiC Composites," *J. Comp. Mater.,* 1992, *26*(14), pp. 2076-106.
16. M. Hayashi and N. Tatsumoto: "Processing and Mechanical Properties of SiC Particle Dispersion Strengthened AC8A Composites by Agitating Casting," *J. Japan Foundrymen's Soc.,* 1993, *65*(11), pp. 846-52.
17. Y.H. Seo and C.G. Kang: "The Effect of Applied Pressure on Particle-Dispersion Characteristics and Mechanical Properties in Melt Stirring Squeeze Cast SiCp/Al Composites," *J. Mater. Processing Technol.,* 1995, *55*, pp. 370-79.
18. T. Yamauchi and Y. Nishida: "Infiltration Kinetics of Al-12%Si Alloy into SiC Whiskers Preform," *J. Japan Inst. Met.,* 1994, *58*(12), pp. 1436-43.
19. H.K. Jung and C.G. Kang: "An Induction Heating Process with Coil Design and Solutions Avoiding Coarsening Phenomena of Al-6 pct Si-3 pct Cu-0.3 pct Mg Alloy for Thixoforming," *Metall. Mater. Trans. A,* 1999, *30A*(11), pp. 2967-77.
20. H.K. Jung, C.G. Kang, and Y.H. Moon: "Induction Heating of Semi-Solid Billet and Control of Globular Microstructure to Prevent Coars-

ening Phenomena," *J. Mater. Eng. Performance,* 2000, *9*(1), pp. 12-23.
21. H.K. Jung and C.G. Kang: "Reheating Process of Cast and Wrought Aluminium Alloys for Thixoforging and Their Globularization Mechanism," *J. Mater. Processing Technol.,* 2000, *104*(3), pp. 244-53.
22. H.K. Jung and C.G. Kang: "Finite Element Numerical Simulation Modeling for Reheating Process of Semi-Solid Forming," *Key Eng. Mater.,* 2000, *177-180*, pp. 571-76.
23. H.K. Jung and C.G. Kang: "Advanced Numerical Simulations of Semi-Solid Forming Process," *Proc. 8th Int. Symp. on Plasticity and Its Current Applications (PLASTICITY2000),* Whistler Resort, Vancouver, 2000, A.S. Khan, ed., Whistler Resort, Vancouver, 2000, pp. 240-42.
24. E.J. Davies: *Conduction and Induction Heating,* Peter Peregrinus Ltd., London, 1990, pp. 100-222.
25. N.R. Stansel: *Induction Heating,* McGraw-Hill, New York, 1949, p. 178.
26. *Metals Handbook,* 10th ed., vol. 2, ASM International, Materials Park, OH, 1990, pp. 164-6 and 1020-2.
27. S.S. Ahn, C.G. Kang, and H.H. Jo: "Induction Heating of Metal Matrix Composites for Thixoforming," *Proc. 2nd Asia-Australasian Conf. on Composite Materials (ACCM-2000),* Kyongju, 2000, Kyongju, Korea, 2000, pp. 309-14.
28. H.J. Rack: *Processing and Properties of Powder Metallurgy Composites,* The Metallurgical Society, Warrendale, PA, 1988, pp. 155.